

# End-Permian Mass Extinction in the Oceans: An Ancient Analog for the Twenty-First Century?

Jonathan L. Payne<sup>1</sup> and Matthew E. Clapham<sup>2</sup>

<sup>1</sup>Department of Geological and Environmental Sciences, Stanford University, Stanford, California 94305; email: jlpayne@stanford.edu

<sup>2</sup>Department of Earth and Planetary Sciences, University of California, Santa Cruz, California 95064; email: mclapham@es.ucsc.edu

Annu. Rev. Earth Planet. Sci. 2012. 40:89–111

First published online as a Review in Advance on  
January 3, 2012

The *Annual Review of Earth and Planetary Sciences* is  
online at earth.annualreviews.org

This article's doi:  
10.1146/annurev-earth-042711-105329

Copyright © 2012 by Annual Reviews.  
All rights reserved

0084-6597/12/0530-0089\$20.00

## Keywords

ocean acidification, evolution, isotope geochemistry, volcanism,  
biodiversity

## Abstract

The greatest loss of biodiversity in the history of animal life occurred at the end of the Permian Period (~252 million years ago). This biotic catastrophe coincided with an interval of widespread ocean anoxia and the eruption of one of Earth's largest continental flood basalt provinces, the Siberian Traps. Volatile release from basaltic magma and sedimentary strata during emplacement of the Siberian Traps can account for most end-Permian paleontological and geochemical observations. Climate change and, perhaps, destruction of the ozone layer can explain extinctions on land, whereas changes in ocean oxygen levels, CO<sub>2</sub>, pH, and temperature can account for extinction selectivity across marine animals. These emerging insights from geology, geochemistry, and paleobiology suggest that the end-Permian extinction may serve as an important ancient analog for twenty-first century oceans.

## INTRODUCTION

Few events in the history of life pose greater challenges or have prompted more varied speculation than the end-Permian mass extinction [ $\sim 252$  million years ago (Mya)], the greatest biodiversity crisis in the history of animal life. The mass extinction event permanently altered the taxonomic composition and ecological structure of Earth's biota (e.g., Bambach et al. 2002, Sepkoski 1981). Identifying the causes of the end-Permian catastrophe and the controls on subsequent recovery is therefore critical to understanding the origins of modern global ecosystems.

The Permian-Triassic (P-Tr) transition has long been recognized as the post-Cambrian minimum in marine diversity (Phillips 1860), but the possibility that this decline resulted from a global biotic crisis received little attention until Schindewolf (1954) proposed that it was caused by a burst of extraterrestrial radiation. Early quantitative biodiversity compilations revealed the great severity of the end-Permian extinction, but testing between gradual (Newell 1962) and catastrophic (Schindewolf 1954) hypotheses remained beyond the resolution of existing data.

Demonstrations of rapid biodiversity loss during the latest Permian (Changhsingian) emerged during the 1990s. Jin et al. (1994) and Stanley & Yang (1994) showed that diversity losses at the end of the Middle Permian (Capitanian) were distinct and separated by millions of years from the end-Permian (Changhsingian) crisis. A geologically rapid (i.e., less than a few million years) end-Permian biodiversity crisis ruled out any slow-acting process, such as the assembly of Pangaea, as the primary cause of mass extinction. However, many potential extinction mechanisms remained, leading Erwin (1993) to propose that flood basalt volcanism, methane hydrate release, climate change, ocean anoxia, and sea-level fall combined to cause the mass extinction.

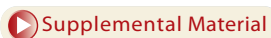
In this review, we address recent paleontological and geochemical findings that place new constraints on the end-Permian extinction. We focus primarily on the better-studied marine record and use a new database of Permian and Early Triassic marine invertebrate occurrences (Clapham et al. 2009), which is freely available in the Paleobiology Database (<http://www.paleodb.org>), to reevaluate marine extinction severity and selectivity. All analyses presented here are based on data downloaded from the Paleobiology Database on July 12, 2011.

## PALEONTOLOGY

### Severity

Despite the severity of the end-Permian extinction and the recognition of a distinct Capitanian crisis (Jin et al. 1994, Stanley & Yang 1994), the partitioning of taxonomic losses between those extinctions has been less certain. Estimates of Capitanian extinction severity using Sepkoski's (2002) compendium suggested that it was comparable in size with the younger end-Permian extinction (e.g., Knoll et al. 2007, Stanley & Yang 1994). However, recent work shows that Sepkoski's database overestimates Capitanian and underestimates Changhsingian extinction magnitude for a number of reasons (Clapham et al. 2009). Our reevaluation of Permian extinctions using an expanded and revised data set shows that genus extinctions were strongly concentrated in the Changhsingian (79% extinction in the Changhsingian versus 24% in the Capitanian; see **Figure 1**) (see also **Supplemental Sidebar 1**, Measuring Diversity and Extinction; access it by following the Supplemental Materials link from the Annual Reviews home page at <http://www.annualreviews.org>).

No major marine invertebrate or protist group escaped the end-Permian extinction unscathed (**Figure 2**), and many invertebrate clades were eliminated entirely. Trilobites, rugose corals, tabulate corals, goniatites, strophomenate brachiopods, blastoids, and rostroconchs occur for the final time in Changhsingian strata, in many cases immediately below the extinction horizon, or in postextinction mixed faunas. Spiriferid and orthid brachiopods (Class Rhynchonellata) also



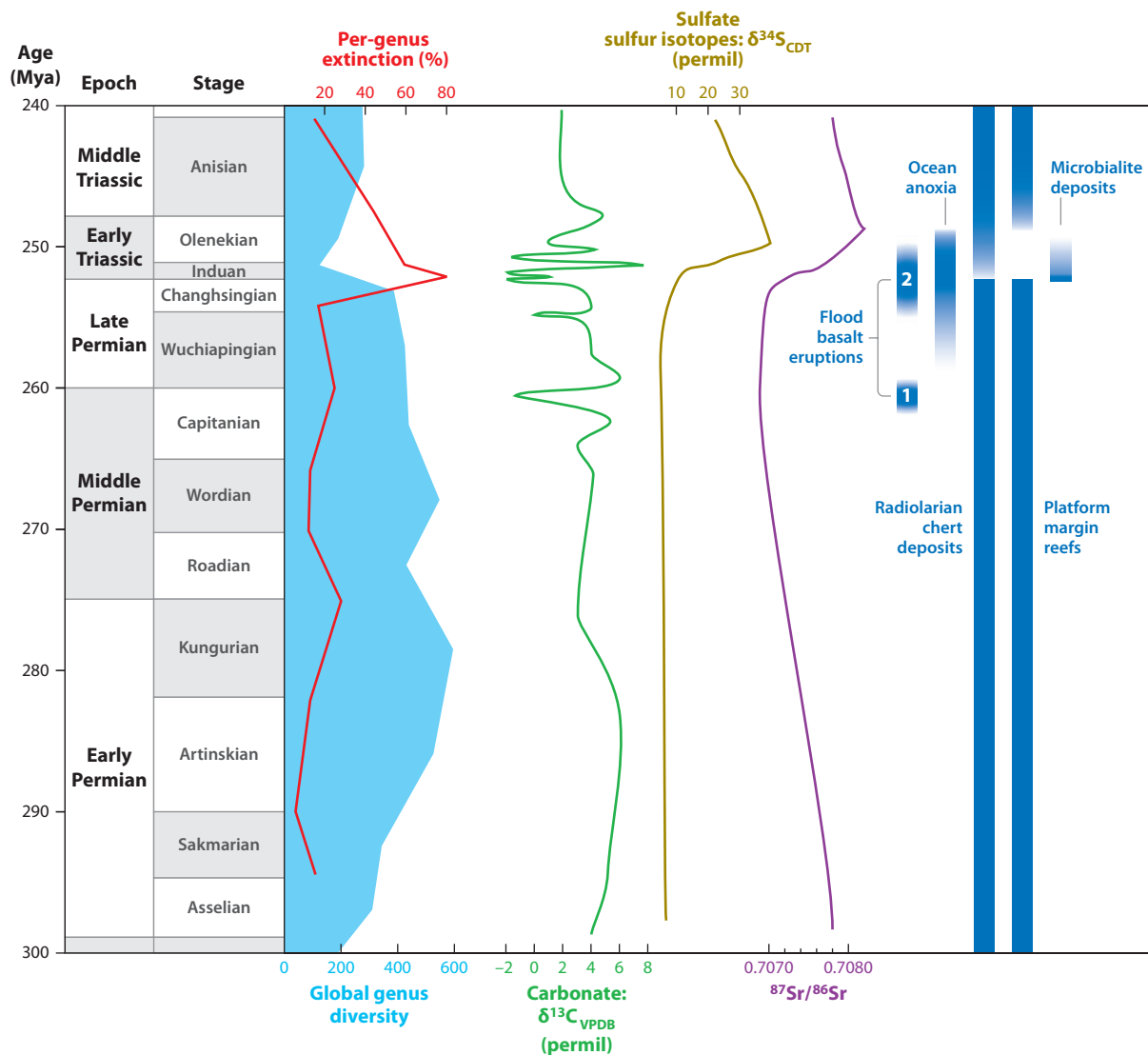


**Figure 1**

Overview of Early Permian through Middle Triassic Earth history, illustrating the coincidence of biological, geochemical, and sedimentary perturbations near the Permian-Triassic (P-Tr) boundary. Global diversity data and extinction rates calculated from the Paleobiology Database using Alroy's (2010) shareholder quorum subsampling (SQS) method. Carbon isotope record based on data from Grossman et al. (2008), Bond et al. (2010), Shen et al. (2010b), and Payne et al. (2004). Sulfur isotope record based on data from Kampschulte & Strauss (2004) and Horacek et al. (2010). Strontium isotope record based on data from McArthur et al. (2001) and Korte et al. (2004). Flood basalts: 1: Emeishan large igneous province; 2: Siberian Traps large igneous province. Abbreviations: CDT, Canyon Diablo Troilite; permil, parts per thousand (‰); VPDB, Vienna Pee Dee Belemnite.

went extinct. Fenestrate bryozoans were victims as well, but all other bryozoan orders survived (Powers & Pachut 2008). The P-Tr was the time of greatest turnover among crinoid groups; of the five Permian clades (Cladida, Flexibilia, Disparida, Camerata, and Articulata), only the articulates survived (Twitchett & Oji 2005). The extinction was severe (91% genus loss) for all calcified orders of foraminifera (Lagenida, Miliolida, and Fusulinida), but particularly so for the large and

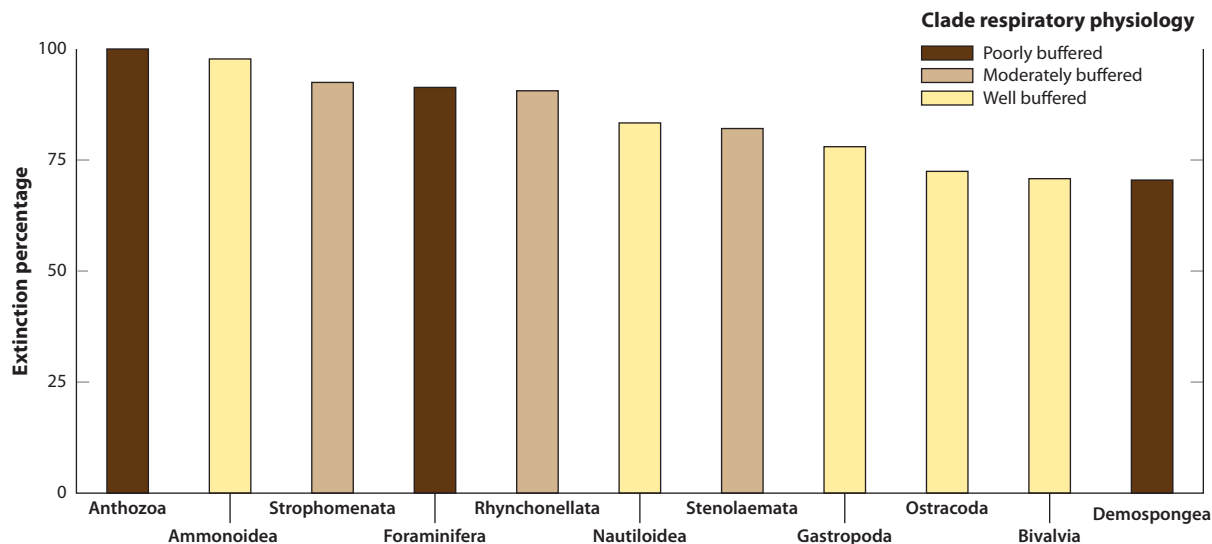


**Figure 2**

Physiological selectivity of the end-Permian extinction. Clades with poorly buffered respiratory physiology are shaded dark brown, moderately buffered clades are in brown, and well-buffered clades are in light yellow. Invertebrate extinctions are calculated as a raw percentage on the basis of all Changhsingian genera from Paleobiology Database data; foraminiferan extinction is also a raw percentage from Groves & Altiner (2005).

morphologically complex superfamily Fusulinoidea, which suffered complete extinction (Groves & Altiner 2005). Radiolarians also suffered major genus-level extinctions (Feng et al. 2007, Kozur 1998), although Paleozoic holdover taxa occur at many sites (Sano et al. 2010) and members of Triassic genera have been found in the latest Permian faunas (Feng et al. 2007, Sano et al. 2010).

The end-Permian extinction was particularly severe for reef organisms and ecosystems. More than 70% of Changhsingian sponge genera were lost, a number that may be artificially low owing to homeomorphy of unrelated Permian and Triassic taxa (Flügel 2002). The complete extinction of rugose and tabulate corals and the appearance and increasing ecological importance of scleractinian corals in Middle and Late Triassic reefs were other key differences between Permian and Triassic reefs (Flügel 2002). The ecological severity of the extinction was even more pronounced; diverse upper Changhsingian hypercalcified sponge-microbe reef ecosystems collapsed abruptly (Flügel & Kiessling 2002) and were replaced by microbialite reefs in the Early Triassic (Baud et al. 2007, Kershaw et al. 2012, Lehrmann et al. 2003).

Less is known about genus-level extinction severity among algae. The diversity of dasycladacean green algae was notably lower in the Triassic than in the Permian (Aguirre & Riding 2005), but Changhsingian genus-level extinction was only 43% (6/14) (calculated from data compiled by Granier & Grgasovic 2000). The relevance of extinction intensity in algae is unclear, however, because many algal genera are morphologically simple and long ranging. Despite these comparatively low taxonomic losses, the near-complete absence of calcareous algae from the Early Triassic fossil record (Aguirre & Riding 2005) indicates that P-Tr environmental conditions strongly affected these organisms.

Palynological data indicate a rapid terrestrial crisis synchronous with the marine event, including decimation of the gymnosperm flora and replacement by opportunistic lycopods (Hochuli et al. 2010, Shen et al. 2011, Twitchett et al. 2001). Blooms of organic-walled microfossils have

been interpreted as a fungal spike following destruction of plant communities (Visscher et al. 1996, 2011), but the taxonomic position of these fossils has been debated and an algal affinity has also been advocated (Foster et al. 2002).

A discrete, global end-Permian mass extinction event is less clearly demonstrated in the vertebrate and plant macrofossil records (Fröbisch 2008, Maxwell 1992, Rees 2002, Xiong & Wang 2011). Global compilations of terrestrial vertebrate diversity also indicate equally high extinction intensity in earlier or later time intervals (e.g., Maxwell 1992). Sections in Russia and the Karoo basin (South Africa), the best-documented regions, display a major extinction at the P-Tr boundary (Benton et al. 2004, Ward et al. 2005), at least broadly equivalent to the marine crisis, but also show elevated extinction in earlier intervals (Benton et al. 2004). Tetrapod extinctions in the Karoo basin are consistent with an abrupt crisis (Ward et al. 2005), but the precise synchronicity with the marine extinction is still unknown because of problematic lithological correlations (Gastaldo et al. 2009) and the questionable validity of correlations based on organic carbon  $\delta^{13}\text{C}$  (Korte & Kozur 2010).

## Selectivity

The end-Permian extinction disproportionately affected certain marine animal clades, a distinction that largely defines the differences between members of Sepkoski's (1981) Paleozoic and Modern faunas. Physiological differences between the two faunas, particularly the varying degrees of stenotopy and eurytopy between brachiopods (Paleozoic fauna) and bivalves (Modern fauna), were initially proposed as a potential explanation for the differential severity of the extinction (e.g., Steele-Petrović 1979), although data available at the time did not permit statistical testing. Later, Rhodes & Thayer (1991) found no significant association between trophic mode or locomotor type and extinction risk across bivalve genera during the end-Permian mass extinction, in marked contrast to the corresponding association during the end-Cretaceous extinction. Knoll et al. (1996) used Sepkoski's genus compendium to examine extinction selectivity across marine animals and protists in terms of predicted susceptibility to hypercapnia, finding greatly elevated extinction rates in the taxa most susceptible (e.g., corals, brachiopods, echinoderms). Knoll et al. (2007) further found that heavily skeletonized groups, such as corals, suffered more in the extinction and argued that hypercapnic stress from elevated  $p\text{CO}_2$  could best account for extinction selectivity even if anoxia, hydrogen sulfide, and temperature change also contributed to the severity through synergistic effects on respiratory physiology. The same suite of stresses may also account for the ecological structure of Early Triassic marine communities (Fraiser & Bottjer 2007, Knoll et al. 2007). The importance of respiratory physiology has been confirmed in studies of the Paleobiology Database (Clapham & Payne 2011, Kiessling & Simpson 2011), and multiple regression analysis shows that both physiological buffering capacity and shell mineralogy are significant predictors of survivorship, even after accounting for the effects of geographic range, abundance, and life position (Clapham & Payne 2011).

In contrast to the strong influence of individual-level traits such as physiology, population-level traits played only a weak role in end-Permian survivorship. Local or global abundance did not favor survival (Clapham & Payne 2011, Leighton & Schneider 2008), and the effects of wide geographic range, usually a strong predictor of survival, were greatly weakened in the end-Permian extinction (Clapham & Payne 2011, Payne & Finnegan 2007). Extinction severity was remarkably uniform among different regions within Tethys, as well as at high northern and southern latitudes (**Figure 3**). Extinctions in south China deviate slightly from the otherwise spatially homogeneous pattern owing to the short-term survival of the most common brachiopod taxa in postextinction mixed faunas (Chen et al. 2005).

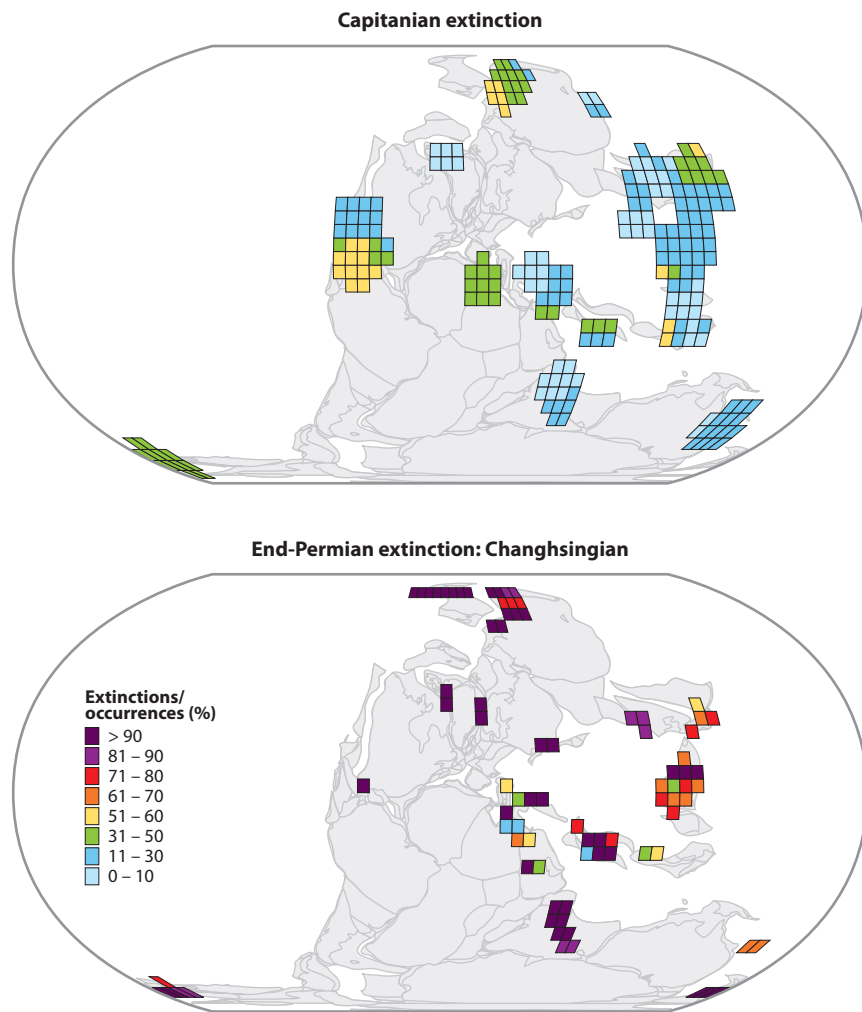


**Figure 3**

Geographic selectivity of Capitanian and end-Permian extinctions, using a kernel density function that compares the number of occurrences of extinct genera against the total number of occurrences. The end-Permian extinction was extremely severe in all regions, such as Tethys, peri-Gondwana, and at high northern and southern latitudes, in contrast with the Capitanian extinction, which had considerable spatial variability owing to sedimentary record loss (Clapham et al. 2009).

There is no evidence for variation in extinction intensity across environmental gradients. Chen et al. (2011) documented 72–92% extinction among brachiopod genera in six different habitats from nearshore to bathyal regions in south China. Although the 92% genus extinction in the reef habitat was higher than in other habitats, the among-habitat differences are not statistically significant.

### Timing and Tempo of Extinction

Studies of classic P-Tr boundary sections in Kashmir, India (Nakazawa et al. 1975), south China (Sheng et al. 1984), and Italy (Broglio Loriga et al. 1986) demonstrated that extinctions

were concentrated in a narrow stratigraphic interval in the latest Changhsingian. Intensified investigation of P-Tr boundary sections in the past decade is beginning to allow detailed comparison across regions to determine whether diversity losses were globally synchronous.

Constraints on the absolute age of the end-Permian extinction derive primarily from the Meishan and Shangsi sections in south China, where volcanic ash layers are intercalated within uppermost Permian and lowermost Triassic carbonates. Improved preparation methods to etch damaged parts of zircons that suffered lead loss and exclusive use of single-crystal analyses yield ages of  $252.4 \pm 0.3$  Mya (Mundil et al. 2004) and  $252.28 \pm 0.08$  Mya (Shen et al. 2011) for Meishan bed 25, which agree within error.

The main pulse of the end-Permian extinction was synchronous across south China, the best-studied region (**Figure 4**), beginning at the top of the *Clarkina yini* zone, before the biostratigraphically defined P-Tr boundary, and extending into the basal Triassic *Hindeodus parvus* zone (J. Chen et al. 2009, Ji et al. 2007, Shen et al. 2011). Combining geochronologic constraints with fossil ranges from well-studied sections in south China shows that biodiversity loss occurred as a single pulse beginning at 252.30 Mya and ending by 252.10 Mya (Shen et al. 2011). These findings are consistent with evidence for abrupt extinction of foraminifera in Italy (Groves et al. 2007, Rampino & Adler 1998) and Turkey (Groves et al. 2005) at approximately the same stratigraphic level as those in China. Although short-lived survivor taxa occur in postextinction strata (Chen et al. 2005, Z.-Q. Chen et al. 2009, Posenato 2009), newly compiled data indicated that an apparent multiphase extinction (Yin et al. 2007) reflects sampling effects rather than truly discrete crises (Shen et al. 2011).

Assessment of synchronicity at wider scales is complicated by facies specificity of important conodont index fossils (Farabegoli et al. 2007) and by the limits of conodont biostratigraphic correlation and resolution (Shen & Mei 2010). In Italy, the main extinction pulse (Groves et al. 2007) occurred within the *H. praeparvus* conodont zone, correlated in part with the *C. meishanensis* zone, potentially implying a slightly diachronous onset of extinction between eastern and western Tethys (Farabegoli et al. 2007, Kozur 2007); however, alternative sequence stratigraphic correlations suggest a synchronous crisis (Posenato 2010). In Iran, the extinction occurred at the top of the *C. hauschkei* zone, most likely correlative to the upper part of the *C. yini* zone at Meishan (Kozur 2007; C. Henderson, personal communication), but it has also been correlated with the younger *meishanensis* zone (Shen & Mei 2010). The timing of the extinction is broadly contemporaneous in peri-Gondwanan localities of Tibet, Spiti, Kashmir, and the Salt Range (Shen et al. 2006); in seamounts in central Neotethys (Shen et al. 2010a); and in the Boreal localities of Greenland and Spitsbergen (Twitchett et al. 2001, Wignall et al. 1998), although precise synchronicity is difficult to prove because conodont occurrences are limited prior to the extinction.

## ENVIRONMENTAL CONTEXT

### Lithological Evidence

Laminated, pyrite-rich lithofacies in P-Tr boundary sediments provided the first evidence for widespread anoxia in shallow-marine environments during the end-Permian extinction (Wignall & Hallam 1992, 1993; Wignall & Twitchett 1996). Common in boundary interval strata is syngenetic pyrite (Wignall & Hallam 1992), which includes small-sized pyrite framboids that suggest anoxic and euxinic (i.e.,  $H_2S$ -bearing) seawater was widespread in Tethyan, eastern Panthalassan, and Boreal sections around the time of the extinction (Bond & Wignall 2010, Nielsen et al. 2010, Shen et al. 2007, Wignall et al. 2005). Framboidal pyrite data suggest development of anoxia and



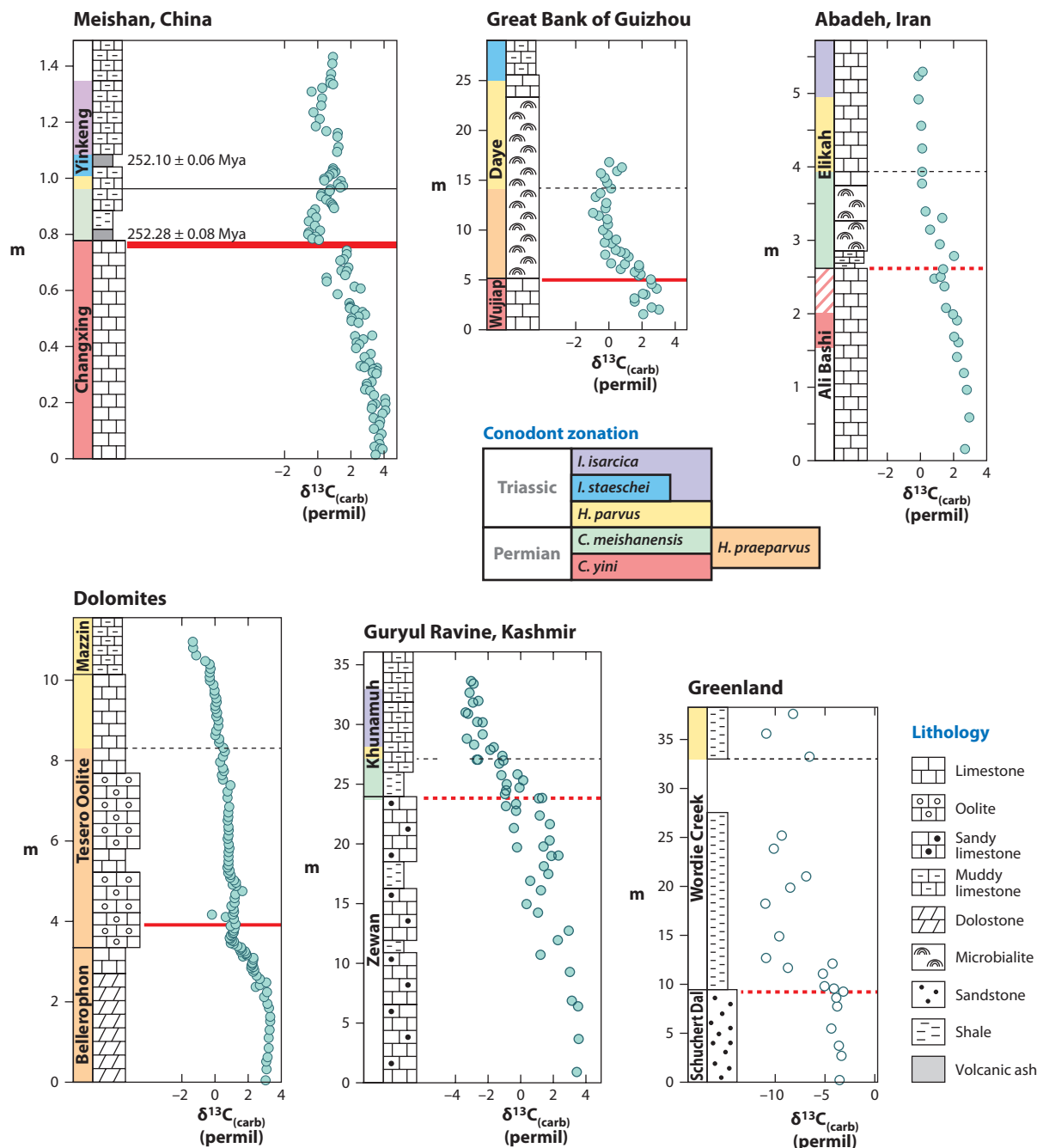


**Figure 4**

Uppermost Changhsingian to lowermost Triassic stratigraphy of selected Permian-Triassic (P-Tr) boundary sections from eastern Tethys (Meishan, Great Bank of Guizhou), western Tethys (Abadeh, Dolomites), peri-Gondwana (Guryul Ravine), and the Boreal realm (Greenland). All vertical scales are in meters. Main extinction pulses are indicated by red lines: solid when constrained by confidence intervals or other quantitative analyses, and dashed when assessed qualitatively. See the **Supplemental Material** for data sources and further explanation. Abbreviations: (carb), carbonate; permil, parts per thousand (‰).



euxinia was also spatially complex (Bond & Wignall 2010), consistent with the lithofacies evidence for diachronous anoxia in P-Tr boundary sections (Wignall & Hallam 1993).

Sediments immediately overlying the extinction horizon are often dominated by microbial buildups (stomatolites and thrombolites; **Figures 4 and 5**) or feature unusual sedimentary textures such as decimeter-scale crystal fans representing seafloor carbonate precipitates (e.g., Baud et al. 2007, Kershaw et al. 2007). These facies are most widespread within the basal Triassic *H. parvus* conodont zone, occurring in south China, western Tethys, Panthalassa, Greenland, and Australia (reviewed in Kershaw et al. 2012). Crusts and mounds composed of crystal fans are best developed in western Tethys localities (Baud et al. 2007). The development and preservation of microbial facies in the aftermath of the extinction have been attributed to a reduction in metazoan grazing and bioturbation (Lehrmann et al. 2003, Pruss & Bottjer 2004), upwelling of alkaline deep waters supersaturated with calcium carbonate (Kershaw et al. 2007, Lehrmann et al. 2003), and increased carbonate deposition in the aftermath of an ocean acidification event (Payne et al. 2007, 2010).

## Carbon Isotopes

One of the first documented geochemical features of P-Tr boundary strata was a perturbation of the global carbon cycle. In the best-studied marine sections with the longest temporal records,  $\delta^{13}\text{C}$  values typically exhibit a gradual decline from near +4‰ to closer to +2‰ near the extinction horizon (**Figures 4 and 5**). The  $\delta^{13}\text{C}$  excursion has now been documented at more than 100 marine localities and numerous nonmarine sections and has been observed in carbonate sediments, bulk organic matter, and individual organic compounds (reviewed by Korte & Kozur 2010). Near the extinction horizon, values decline more rapidly to a minimum typically near -1‰ or -2‰ before returning to (temporarily) stable values between +1‰ and +2‰. The interval of extremely depleted  $\delta^{13}\text{C}$  values coincides approximately with the basal Triassic *H. parvus* conodont zone. There may be two or more cycles between more enriched and more depleted  $\delta^{13}\text{C}$  values during the earliest Triassic (Holser et al. 1989, Xie et al. 2007).

Two classes of explanation have been proposed for the  $\delta^{13}\text{C}$  excursion: (a) collapse of primary productivity and the resulting isotopic homogenization of the oceans (known as a Strangelove Ocean) (e.g., Erwin et al. 2002, Rampino & Caldeira 2005) and (b) addition of  $^{13}\text{C}$ -depleted carbon to the oceans and atmosphere (known as a carbon injection). Carbon depleted in  $^{13}\text{C}$  could derive from methane clathrates (e.g., Erwin 1993), methane dissolved in deep ocean waters (Ryskin 2003), dissolved inorganic carbon in the deep waters of a stratified ocean (e.g., Kajiwarra et al. 1994, Knoll et al. 1996), a large dissolved marine organic carbon reservoir (Rothman 2010), or sedimentary organic carbon deposits (e.g., Svensen et al. 2004). In the Strangelove Ocean scenario, the isotope excursion is a consequence of extinction, whereas in the carbon injection scenario it is linked to the cause.

Carbon injection and the Strangelove Ocean are not mutually exclusive, but two lines of evidence suggest carbon injection was the more important control on the carbon isotope record. First, there appears to have been a substantial depth gradient in  $\delta^{13}\text{C}$  values shortly following the mass extinction event (Meyer et al. 2011), contrary to the isotopic homogenization predicted under the Strangelove Ocean scenario. Second, the boundary  $\delta^{13}\text{C}$  excursion was not an isolated event; rather, it was part of a series of large positive and negative excursions that began during Permian time and persisted through the Early Triassic (**Figure 1**).

Although most authors have interpreted the boundary  $\delta^{13}\text{C}$  excursion to result from carbon injection, the magnitude and isotopic composition of the released carbon are unknown because they cannot be uniquely constrained by the magnitude of the  $\delta^{13}\text{C}$  excursion alone. Berner (2002) argued that the amount of carbon required from any source isotopically heavier than biogenic

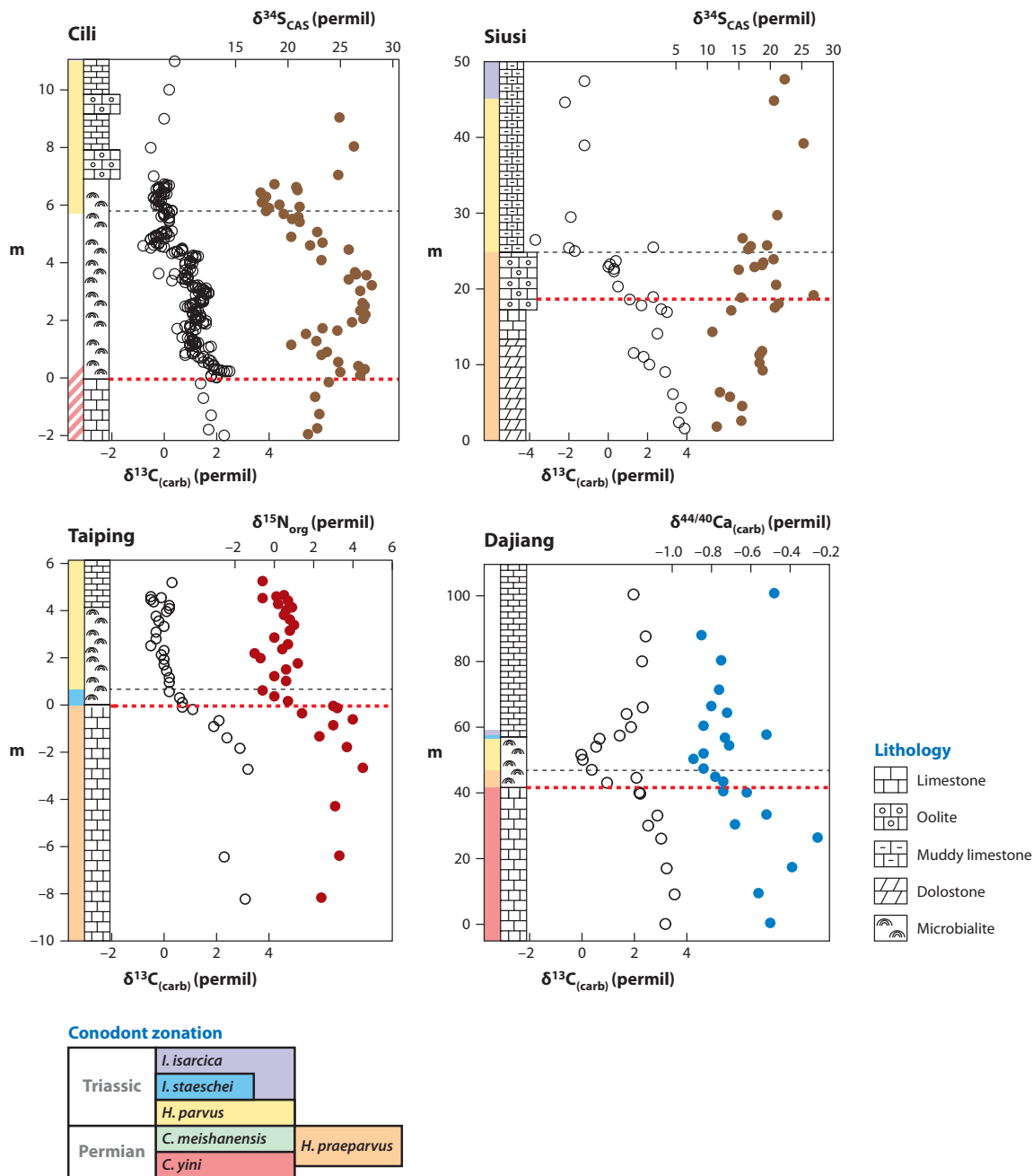



**Figure 5**

Coupled isotope records from representative Permian-Triassic (P-Tr) boundary sections. Cili section from Luo et al. (2010); Siusi section from Newton et al. (2004); Taiping section from Luo et al. (2011); Dajiang section from Payne et al. (2010). All symbols as in **Figure 4**. Cross-hatched pattern in the conodont zonation for lower Cili section indicates constraints based on foraminifera, and carbon isotopes suggest correlation with the *Clarkina yini* zone. Conodont zonation for Dajiang is based on correlative strata at Heping (Krull et al. 2004) and Dawen (J. Chen et al. 2009), on the same carbonate platform. Error bars on calcium isotope values indicate one standard deviation based on replicate measurements. Abbreviations: (carb), carbonate; CAS, carbonate-associated sulfate; org, organic.

methane ( $-60\%$ ) was implausibly large. However, recent work on volcanic interactions with organic carbon in sedimentary basins suggests that volcanism can induce the volatilization of much larger quantities of carbon from sedimentary strata than had previously been appreciated (e.g., Svensen et al. 2009), opening the possibility that at least some carbon was derived from other pools.

## Calcium Isotopes

Calcium isotope ( $\delta^{44/40}\text{Ca}$ ) records have the potential to further constrain interpretations of carbon cycling because the two cycles are linked through the common sink of calcium carbonate burial. The only detailed calcium isotope record across the end-Permian extinction horizon exhibits a negative shift of approximately  $0.3\%$  in the micrite fraction of bulk carbonate rock (**Figure 5**). This excursion could reflect either a global shift in the proportion of aragonite versus calcite deposition (because these two polymorphs of  $\text{CaCO}_3$  fractionate calcium isotopes differently relative to seawater) or a rapid increase in the calcium concentration of seawater, likely resulting from ocean acidification (Payne et al. 2010). If the latter scenario applies, variation in  $\delta^{44/40}\text{Ca}$  values can be used to constrain the isotopic composition of injected carbon. The  $0.3\%$  excursion in  $\delta^{44/40}\text{Ca}$  values suggests injected carbon  $\delta^{13}\text{C}$  values near  $-15\%$  and no lighter than  $-30\%$  (see **Supplemental Sidebar 2**, Interpreting the P-Tr Boundary Carbon Isotope Excursion), ruling out biogenic methane as the sole source of injected carbon (Payne et al. 2010). Records from additional localities are required to determine the extent to which this signal is globally reproducible and whether it is likely to reflect a shift in the  $\delta^{44/40}\text{Ca}$  of seawater.

 [Supplemental Material](#)

## Sulfur Isotopes

Similar to carbon isotope records, sulfur isotope records exhibit substantial variations near the end-Permian extinction and through the P-Tr transition more broadly. A long-term positive shift in  $\delta^{34}\text{S}$  values of sulfate evaporites from  $+12\%$  to  $+28\%$  between the Late Permian and the late part of the Early Triassic (**Figure 1**) has been established for several decades (e.g., Cortecchi et al. 1981). More recently, analysis of  $\delta^{34}\text{S}$  variation in pyrite and carbonate-associated sulfate has opened the possibility of examining sulfur cycle behavior at high resolution across the P-Tr boundary interval.

High-resolution sulfur isotope records from sedimentary pyrite and carbonate-associated sulfate typically exhibit variation of tens of permil (parts per thousand;  $\%$ ), often between stratigraphically adjacent samples (**Figure 5**; see also Algeo et al. 2008, Fenton et al. 2007, Gorjan et al. 2007, Kaiho et al. 2001, Kajiwarra et al. 1994, Luo et al. 2010, Newton et al. 2004, Nielsen et al. 2010, Riccardi et al. 2006).

Interpretations of P-Tr boundary sulfur cycle dynamics from isotope records have focused on two possibilities: mixing of isotopically distinct and physically separated reservoirs and variation in the isotopic composition of the entire ocean sulfur reservoir. The rapidity and magnitude of the sulfur isotope excursions have led many authors to favor the former possibility. Kajiwarra et al. (1994) and many subsequent authors (e.g., Algeo et al. 2008, Newton et al. 2004, Riccardi et al. 2006) proposed that isotopically distinct sulfur pools were segregated vertically in a stratified ocean, with negative isotope excursions in shallow-marine sections reflecting upwelling of waters from below the chemocline. In contrast, Luo et al. (2010) interpreted the excursions to reflect variation in the proportional burial of pyrite versus sulfate in an ocean with low sulfate concentrations ( $<1\text{ mM}$ ). Kaiho et al. (2001) suggested that the negative shift resulted from a massive addition of  $^{34}\text{S}$ -depleted sulfur from the mantle, which was released during a massive bolide impact.

The implications of the impact scenario (Kaiho et al. 2001) are implausible, requiring an asteroid of 30–60 km in diameter or a comet of 15–30 km in diameter, a resulting crater of 600–1,200 km, and a postimpact ocean pH of 1.5–2.5, the latter of which would likely have killed nearly all invertebrate animals. Oxidation of the sulfur would have consumed as much as 40% of the atmospheric O<sub>2</sub> reservoir.

Distinguishing between the upwelling and low-sulfate scenarios remains a challenge, as both explain large-amplitude, short-term variation in  $\delta^{34}\text{S}$  values as well as correlation between the  $\delta^{13}\text{C}$  and  $\delta^{34}\text{S}$  records (Algeo et al. 2008, Luo et al. 2010). Because the upwelling scenario is inherently of local-to-regional scale, the demonstration of correlative excursions at a global scale would point toward the low-sulfate scenario. However, determining whether features of the  $\delta^{34}\text{S}$  record are indeed correlative across widely separated sections is challenging because many occur on timescales shorter than those resolved by biostratigraphy.

## Nitrogen Isotopes

Decrease in the nitrogen isotopic ( $\delta^{15}\text{N}$ ) composition of organic carbon across the end-Permian extinction horizon suggests an increased proportional contribution of nitrogen fixers (e.g., cyanobacteria) to preserved organic matter.  $\delta^{15}\text{N}$  values exhibit a negative shift of approximately 3‰ at Meishan (Cao et al. 2009) and in two shallow-marine sections from the Nanpanjiang Basin of south China (Luo et al. 2011) (**Figure 5**). In contrast,  $\delta^{15}\text{N}$  values show little variation across the boundary interval at the Guryul Ravine section of Kashmir (Algeo et al. 2007). Decreases in  $\delta^{15}\text{N}$  values and enhanced nitrogen fixation are predicted under conditions of widespread marine anoxia and consistent with many other lines of evidence (e.g., Isozaki 1997, Wignall & Twitchett 2002).

## Organic Geochemistry

Organic geochemical analysis has provided important confirmation of shallow-marine anoxia. Isorenieratane and aryl isoprenoids (molecular fossils derived from isorenieratene, a photosynthetic pigment produced by green sulfur bacteria) occur in P-Tr boundary sediments at Meishan and in the Hovea-3 core (Grice et al. 2005). Because green sulfur bacteria require sunlight and hydrogen sulfide to conduct photosynthesis, this finding supports interpretations of shallow-marine anoxia and euxinia around the time of the main extinction pulse. Cao et al. (2009) recovered isorenieratane at many stratigraphic levels within Changhsingian strata at Meishan, suggesting that photic-zone euxinia developed at least intermittently through Changhsingian time, long prior to the main extinction event. Thus, if anoxia was a cause of extinction, it must have surpassed a threshold of biological tolerance during the latest Changhsingian. However, the co-occurrence of abundant isorenieratane with diverse benthic invertebrate assemblages suggests that green sulfur bacteria may have thrived during intervals, perhaps seasonal, of photic-zone euxinia that were neither extensive nor prolonged enough to significantly impact animal communities. Alternatively, the occurrence of seafloor microbialites in the boundary interval at Meishan (Cao & Zheng 2009) and in the Hovea-3 core (Thomas et al. 2004) opens the possibility that the biomarkers derive from photosynthetic seafloor microbial mats rather than organisms living within a euxinic water column. The former possibility is consistent with recently reported uranium isotope evidence for an expansion of ocean anoxia coincident with the mass extinction event (Brennecke et al. 2011).

Biomarker data also point toward an increase in the proportional contribution of microbial biomass to organic deposits through the boundary interval. At Meishan, increases in the abundances of 2-methylhopanes relative to other hopanes, and of hopanes relative to steranes (Xie et al. 2005), have been interpreted to reflect increased cyanobacterial contribution to primary production and overall changes to microbial community composition (Cao et al. 2009). However, recent

genetic and phylogenetic work shows that other bacterial groups also produce 2-methylhopanoids, limiting the utility of this molecule as a cyanobacterial biomarker (Welander et al. 2010).

Organic geochemical data from marine sections have also been interpreted to reflect the collapse of terrestrial ecosystems. Dibenzofurans and other polycyclic aromatic hydrocarbons occur in elevated abundance in Upper Permian strata from China, Italy, and Greenland (Fenton et al. 2007, Sephton et al. 2005, Wang & Visscher 2007), possibly reflecting increased contributions of soil organic carbon and even catastrophic collapse of the terrestrial flora (e.g., Sephton et al. 2005). However, Grice et al. (2007) observed a negative excursion in the  $\delta^{13}\text{C}$  of these molecules across the P-Tr boundary within the Hovea-3 core. Permian  $\delta^{13}\text{C}$  values are consistent with a terrestrial source, whereas Triassic values are more consistent with a marine source, likely algae. Cao et al. (2009) argued that long-term organic records indicate lithological and diagenetic controls on the abundances of these molecules, rather than indicating denudation of the land surface. Consequently, the extent to which the organic geochemical record reflects terrestrial ecosystem collapse remains uncertain.

## SUMMARY OF PATTERN

Any successful explanation for the end-Permian mass extinction must account for the following observations. First, the extinction was the most severe biotic crisis of the Phanerozoic, affecting both marine and terrestrial ecosystems. Second, the main extinction pulse occurred over a timescale shorter, and likely much shorter, than a few hundred thousand years. Third, marine animals with limited physiological capacity to buffer themselves against changes in ambient  $p\text{CO}_2$ , temperature, pH, and oxygen concentration were preferentially victimized. Fourth, sedimentary fabrics, pyrite framboid abundances, and organic biomarkers suggest widespread ocean anoxia and euxinia that reached shallow-marine habitats at least episodically, beginning during Changhsingian time but peaking in intensity around the main extinction pulse. Fifth, the  $\delta^{13}\text{C}$  composition of carbonate rocks and organic carbon began to decrease shortly before the main extinction pulse and dropped most abruptly, coincident with the mass extinction. Sixth, environmental disruption and its biological consequences continued through much of the Early Triassic.

## GEOLOGICAL TRIGGERS

During the past decade, debate over the causes of the end-Permian mass extinction has focused on three geological triggers. These are (a) bolide impact; (b) overturn or upwelling of deep water in a stratified, anoxic ocean; and (c) flood basalt volcanism.

### Bolide Impact

A major bolide impact is consistent with the rapidity and magnitude of the mass extinction, but it does not easily explain the selectivity against physiological traits rather than dietary traits, the evidence for persistent ocean anoxia, or the long-term perturbations recorded by carbon and sulfur isotopes.

Beyond these issues, the geological and geochemical evidence for bolide impact has been strongly challenged. Reports of fullerene molecules trapping helium and argon with extraterrestrial isotopic compositions (Becker et al. 2001) have not been reproduced in independent analyses of the same samples (Farley & Mukhopadhyay 2001) or from additional P-Tr boundary localities (Farley et al. 2005, Koeberl et al. 2004). A subsurface feature off the coast of Australia interpreted by Becker et al. (2004) as an end-Permian impact crater has been similarly challenged on the basis of poorly constrained age (Renne et al. 2004) and the absence of tsunami-type deposits at the P-Tr

boundary in nearby sedimentary basins (Wignall et al. 2004). The unusually pristine condition of meteorite fragments at the P-Tr boundary in terrestrial deposits from Australia (Basu et al. 2003) has raised questions regarding the likelihood that such grains could be preserved unaltered (French & Koeberl 2010). Subsequent attempts to identify additional meteorite grains from the original samples have so far failed (reported in French & Koeberl 2010). Overall, this paucity of evidence for impact stands in stark contrast to the plenitude of evidence that has emerged at the Cretaceous-Paleogene boundary (Schulte et al. 2010) and suggests that bolide impact is unlikely to have caused the end-Permian mass extinction.

## Ocean Anoxia and Euxinia

Intrusion of oxygen-depleted waters into shallow-marine habitats at the end of the Permian can account for extinction rate and magnitude, assuming end-Permian ocean anoxia was more pervasive or prolonged than other ocean anoxic events. It can also explain the deposition of laminated sediments, small framboids, and biomarkers for green sulfur bacteria, as well as short- and long-term perturbation of the carbon and sulfur isotope records.

However, anoxia and euxinia alone are insufficient to account for several aspects of end-Permian global change. In isolation, anoxia and euxinia would be unlikely to cause the observed pattern of physiological selectivity (Knoll et al. 2007) and the lack of selectivity across environments (Chen et al. 2011). Furthermore, persistent shallow-marine anoxia could be sustained only in areas of upwelling because wind mixing tends to keep the surface ocean in near equilibrium with atmospheric composition (Meyer et al. 2008). Shallow-marine anoxia or euxinia could not have been both temporally persistent and geographically widespread unless atmospheric oxygen levels were far lower than the values indicated by model reconstructions (e.g., Berner 2006). Similarly, global ocean biogeochemical models suggest that deep-marine anoxia is maintained by high nutrient levels in seawater and that scenarios involving simple overturn of a stratified ocean with CO<sub>2</sub>- and H<sub>2</sub>S-charged deep waters are physically unrealistic (e.g., Meyer et al. 2008). Finally, the mechanism by which ocean anoxia and euxinia could cause simultaneous terrestrial and marine extinctions (Twitchett et al. 2001) remains poorly understood. Hydrogen sulfide release from the ocean to the atmosphere was proposed as a link between the two (Kump et al. 2005), but more recent 3D models (Harfoot et al. 2008) suggest that the required magnitude of sulfur release is higher than that proposed by Kump et al. (2005) and that the rate of release of H<sub>2</sub>S from the oceans is less than required owing to biological utilization of reduced sulfur in the surface ocean (Meyer et al. 2008). Low sulfur concentrations in P-Tr seawater (Luo et al. 2010) would further reduce the likelihood that H<sub>2</sub>S release factored in terrestrial extinctions.

Although end-Permian scenarios triggered by overturn of a stratified, anoxic and euxinic ocean continue to be advocated (Şengör & Atayman 2009), the currently more common view is that ocean anoxia and euxinia were sustained via high productivity in a nutrient-rich ocean (e.g., Meyer et al. 2008). These biogeochemical conditions may have contributed to the severity of marine extinctions but were neither the ultimate trigger of the catastrophe nor the only proximal cause of population collapse (e.g., Erwin 2006, Knoll et al. 2007, Meyer & Kump 2008, Wignall 2001).

## Flood Basalt Volcanism

Recent advances in understanding the volcanism of the Siberian Traps suggest that emplacement of this large igneous province (> 5 million km<sup>3</sup> of basalt intruded into the Tunguska Basin of central Russia) can account for nearly all features associated with the end-Permian mass extinction.

First, eruption of the Traps can explain the timing of the extinction event. Radiometric evidence that emplacement of the Siberian Traps was broadly coeval with marine extinctions has existed



for two decades (Renne et al. 1995), but increasingly precise dating of both the basalts and the mass extinction has greatly strengthened the case for synchronicity (Kamo et al. 2003, Mundil et al. 2004, Reichow et al. 2009, Shen et al. 2011).

Second, the unparalleled magnitude of the extinction event can be accounted for by Traps eruptions. The Siberian Traps (including extensive basalts in the subsurface of the West Siberia Basin) constitute one of the largest, if not the largest, continental flood basalt provinces that erupted during Phanerozoic time (Reichow et al. 2002, Wignall 2001). Beyond the simple volume of the Siberian Traps, increasing recognition of the extent of interaction between the basalts and sedimentary rocks in the Tunguska Basin has strengthened the case that the basalt eruptions could have released a sufficient quantity of volatiles to disturb climate as well as atmospheric and ocean chemistry and thereby cause mass extinction. Campbell et al. (1992) recognized that extensive interaction between basalts and anhydrite in the sedimentary cover of the Tunguska Basin could have led to massive release of sulfur volatiles into the upper stratosphere. They hypothesized that resulting global cooling, ice sheet growth, and sea-level fall could account for the mass extinction. However, there is no evidence for glaciation at this time. Svensen et al. (2004) hypothesized that degassing of carbon from organic deposits could also have resulted in massive CO<sub>2</sub> release. Svensen et al. (2009) illustrated the numerous gas explosion structures near the margins of the Siberian Traps and interpreted them to reflect catastrophic gas release events owing to overpressure in the subsurface when magma volatilized sedimentary country rock. They calculated that Traps eruptions could have released more than 30,000 GT (1 GT = 10<sup>15</sup> g) of carbon into the atmosphere, more than five times as much as past and estimated future anthropogenic carbon emissions (Caldeira & Wickett 2003). Comparative analysis suggests not only that the Siberian Traps were the largest continental flood basalt province, but also that they interacted more extensively with volatile-rich country rock than did any other province (Black et al. 2012, Ganino & Arndt 2009).

Third, the release of vast amounts of CO<sub>2</sub> can account for the preferential extinction of heavily calcified marine animals with limited physiological buffering capacity (Knoll et al. 2007), as well as account for the limited selectivity on biogeographic parameters such as geographic range (Clapham & Payne 2011, Payne & Finnegan 2007) or environmental preference (Chen et al. 2011). Although changes in ocean redox state are better recorded than changes in *p*CO<sub>2</sub>, pH, and temperature, we reason that ocean pH, *p*CO<sub>2</sub>, and carbonate saturation state were the more important drivers of extinction. As discussed above, hypoxia and anoxia are difficult to maintain over long timescales in the mixed layer (upper 100–200 m) owing to wind mixing with the large atmospheric oxygen reservoir. In contrast, release of acid volatiles (e.g., CO<sub>2</sub> and SO<sub>2</sub>) would cause reductions in ocean pH and carbonate saturation state even in the surface ocean and may preferentially affect the surface ocean if emitted quickly enough (Caldeira & Wickett 2003). In the absence of a large reservoir of fine-grained, unlithified deep-sea carbonate sediment, whole-ocean acidification could likely last for tens of thousands of years (Archer et al. 1997), and few refugia would exist—survival would depend primarily on long-term physiological tolerance of altered conditions.

Fourth, Siberian Traps volcanism can explain the increased prevalence of marine hypoxia and anoxia associated with the P-Tr boundary interval. Biogeochemical modeling shows that extensive and prolonged marine anoxia requires increased nutrient supply and is maintained by the excess flux of organic carbon relative to oxygen supplied by physical mixing, rather than resulting simply from global warming or a reduction in the rate of physical mixing (Meyer et al. 2008). On geological timescales, phosphate supplied by the chemical weathering of silicate rocks is likely the nutrient that limits productivity in marine systems. An increase in chemical weathering rates on land is predicted on the basis of the Siberian Traps volatile flux and can therefore account for the increased prevalence of ocean anoxia at this time, as well as increased sediment fluxes to marine depositional



systems (Algeo & Twitchett 2010). Beyond explaining marine extinctions, climate change induced by Siberian Traps volatile emissions and possible destruction of the ozone layer by organohalogen release (Svensen et al. 2009, Visscher et al. 2004) may explain the coincident collapses of terrestrial and marine ecosystems.

We hypothesize that ongoing Siberian Traps volcanism during Early Triassic time (Kamo et al. 2003, Reichow et al. 2009) explains the persistence of  $\delta^{13}\text{C}$  excursions (**Figure 1**) and repeated episodes of shallow-marine anoxia (Wignall & Twitchett 2002) and associated evidence of delayed biotic recovery (e.g., Fraiser & Bottjer 2005, Hallam 1991), although the record is not yet sufficiently resolved to quantify rates and magnitudes of magmatic and volatile release within individual substages or biostratigraphic zones. Sustained anoxia can also explain the positive excursion in the  $\delta^{34}\text{S}$  of Early Triassic evaporites through the preferential burial of sulfur as pyrite under euxinic conditions.

## LESSONS FOR THE TWENTY-FIRST CENTURY

As human impacts push environmental conditions to extremes not experienced in the recent past, the geological record is increasingly essential as an archive of past experiments in global change. Carbon release events from the more recent geological past, such as the Paleocene-Eocene Thermal Maximum and other hyperthermal events, allow for more detailed documentation of Earth system changes on short timescales. However, the rates of carbon release associated with these events may have been smaller than those that Earth is currently experiencing (Cui et al. 2011) and so may lead us to underestimate the potential biotic response. The end-Permian rock record cannot currently provide the temporal and spatial resolutions to make specific predictions about expected changes in the coming decades or centuries, but increasing evidence that the end-Permian mass extinction was precipitated by rapid release of  $\text{CO}_2$  into Earth's atmosphere is a valuable reminder that the best—and most sobering—analogs for our near future may lie deeper in Earth's past.

### SUMMARY POINTS

1. The end-Permian mass extinction event eliminated 79% of marine invertebrate genera and had similarly severe effects on the terrestrial biota.
2. The main pulse of extinction was a single, geologically rapid event that occurred over less, and likely much less, than 200,000 years.
3. In the oceans, heavily calcified animals with limited physiological capacity to buffer internal fluid composition against a changing external environment were preferentially victimized.
4. Ocean anoxia was widespread, if episodic, during Changhsingian time. The prevalence of anoxia increased near the time of the main extinction pulse, and widespread anoxia continued, perhaps intermittently, during Early Triassic time. Anoxic and sulfide-bearing waters commonly extended into shallow-marine habitats. Although selectivity patterns appear better explained by the effects of changes in ocean pH,  $p\text{CO}_2$ , and carbonate saturation level, widespread hypoxia would have increased the sensitivity of many organisms to changes in these other environmental parameters.

5. The scenario that best explains these observations invokes the eruption of the Siberian Traps large igneous province as the primary trigger of extinction. Release of volcanic CO<sub>2</sub> as well as volatilized sedimentary organic carbon and evaporite minerals led to global warming, ocean acidification, and perhaps destruction of atmospheric ozone, while enhanced weathering and nutrient runoff exacerbated preexisting ocean anoxia. These Earth system changes caused global population declines and resulted in mass extinction.

## DISCLOSURE STATEMENT

The authors are not aware of any affiliations, memberships, funding, or financial holdings that might be perceived as affecting the objectivity of this review.

## ACKNOWLEDGMENTS

We thank P. Marenco, K. Meyer, and S. Pruss for thoughtful reviews and C. Henderson for assistance with conodont biostratigraphy. This work was supported by the National Science Foundation (EAR-0807377 to J.L.P. and EAR-0918184 to M.E.C.).

## LITERATURE CITED

- Aguirre J, Riding R. 2005. Dasycladalean algal biodiversity compared with global variations in temperature and sea level over the past 350 Myr. *Palaios* 20:581–88
- Algeo T, Shen Y, Zhang T, Lyons T, Bates S, et al. 2008. Association of <sup>34</sup>S-depleted pyrite layers with negative carbonate  $\delta^{13}\text{C}$  excursions at the Permian-Triassic boundary: evidence for upwelling of sulfidic deep-ocean water masses. *Geochim. Geophys. Geosyst.* 9:Q04025
- Algeo TJ, Hannigan R, Rowe H, Brookfield M, Baud A, et al. 2007. Sequencing events across the Permian-Triassic boundary, Guryul Ravine (Kashmir, India). *Palaeogeogr. Palaeoclimatol. Palaeoecol.* 252:328–46
- Algeo TJ, Twitchett RJ. 2010. Anomalous Early Triassic sediment fluxes due to elevated weathering rates and their biological consequences. *Geology* 38:1023–26
- Alroy J. 2010. The shifting balance of diversity among major marine animal groups. *Science* 329:1191–94
- Archer D, Kheshgi H, Maier-Reimer E. 1997. Multiple timescales for neutralization of fossil fuel CO<sub>2</sub>. *Geophys. Res. Lett.* 24:405–8
- Bambach RK, Knoll AH, Sepkoski JJ. 2002. Anatomical and ecological constraints on Phanerozoic animal diversity in the marine realm. *Proc. Natl. Acad. Sci. USA* 99:6854–59
- Basu AR, Petaev MI, Poreda RJ, Jacobsen SB, Becker L. 2003. Chondritic meteorite fragments associated with the Permian-Triassic boundary in Antarctica. *Science* 302:1388–92
- Baud A, Richoz S, Pruss SB. 2007. Lower Triassic anachronistic carbonate facies in space and time. *Global Planet. Change* 55:81–89
- Becker L, Poreda RJ, Basu AR, Pope KO, Harrison TM, et al. 2004. Bedout: a possible end-Permian impact crater offshore of Northwestern Australia. *Science* 304:1469–76
- Becker L, Poreda RJ, Hunt AG, Bunch TE, Rampino M. 2001. Impact event at the Permian-Triassic boundary: evidence from extraterrestrial noble gases in fullerenes. *Science* 291:1530–33
- Benton MJ, Tverdokhlebov VP, Surkov MV. 2004. Ecosystem remodelling among vertebrates at the Permian-Triassic boundary in Russia. *Nature* 432:97–100
- Berner RA. 2002. Examination of hypotheses for the Permo-Triassic boundary extinction by carbon cycle modeling. *Proc. Natl. Acad. Sci. USA* 99:4172–77
- Berner RA. 2006. GEOCARBSULF: a combined model for Phanerozoic atmospheric O<sub>2</sub> and CO<sub>2</sub>. *Geochim. Cosmochim. Acta* 70:5653–64

- Black BA, Elkins-Tanton LT, Rowe MC, Ukstins-Peate I. 2012. Magnitude and consequences of volatile release from the Siberian Traps. *Earth Planet. Sci. Lett.* 317–318:363–73
- Bond DPG, Wignall PB. 2010. Pyrite framboid study of marine Permian-Triassic boundary sections: a complex anoxic event and its relationship to contemporaneous mass extinction. *Geol. Soc. Am. Bull.* 122:1265–79
- Bond DPG, Wignall PB, Wang W, Izon G, Jiang HS, et al. 2010. The mid-Capitanian (Middle Permian) mass extinction and carbon isotope record of South China. *Palaeogeogr. Palaeoclimatol. Palaeoecol.* 292:282–94
- Brennecke GA, Herrmann AC, Algeo TJ, Anbar AD. 2011. Rapid expansion of oceanic anoxia immediately before the end-Permian mass extinction. *Proc. Natl. Acad. Sci. USA* 108:17631–34
- Broglia Loriga C, Neri C, Pasini M, Posenato R. 1986. Marine fossil assemblages from Upper Permian to lowermost Triassic in the western Dolomites (Italy). *Mem. Soc. Geol. It.* 34:5–44
- Caldeira K, Wickett ME. 2003. Anthropogenic carbon and ocean pH. *Nature* 425:365
- Campbell IH, Czamanske GK, Fedorenko VA, Hill RI, Stepanov V. 1992. Synchronism of the Siberian Traps and the Permian-Triassic boundary. *Science* 258:1760–63
- Cao C, Love GD, Hays LE, Wang W, Shen S, Summons RE. 2009. Biogeochemical evidence for euxinic oceans and ecological disturbance presaging the end-Permian mass extinction event. *Earth Planet. Sci. Lett.* 281:188–201
- Cao C, Zheng Q. 2009. Geological event sequences of the Permian-Triassic transition recorded in the microfossils in Meishan section. *Sci. China Ser. D* 52:1529–36
- Chen J, Beatty TW, Henderson CM, Rowe H. 2009. Conodont biostratigraphy across the Permian-Triassic boundary at the Dawen section, Great Bank of Guizhou, Guizhou Province, South China: implications for the Late Permian extinction and correlation with Meishan. *J. Asian Earth Sci.* 36:442–58
- Chen J, Chen Z-Q, Tong J. 2011. Environmental determinants and ecologic selectivity of benthic faunas from nearshore to bathyal zones in the end-Permian mass extinction: brachiopod evidence from South China. *Palaeogeogr. Palaeoclimatol. Palaeoecol.* 308:84–97
- Chen Z-Q, Kaiho K, George AD. 2005. Early Triassic recovery of the brachiopod faunas from the end-Permian mass extinction: a global review. *Palaeogeogr. Palaeoclimatol. Palaeoecol.* 224:270–90
- Chen Z-Q, Tong J, Zhang K, Yang H, Liao Z, et al. 2009. Environmental and biotic turnover across the Permian-Triassic boundary on a shallow carbonate platform in western Zhejiang, south China. *Aust. J. Earth Sci.* 56:775–97
- Clapham ME, Payne JL. 2011. Acidification, anoxia, and extinction: a multiple regression analysis of extinction selectivity during the Middle and Late Permian. *Geology* 39:1059–62
- Clapham ME, Shen S, Bottjer DJ. 2009. The double mass extinction revisited: reassessing the severity, selectivity, and causes of the end-Guadalupian biotic crisis (Late Permian). *Paleobiology* 35:32–50
- Cortecci G, Reyes E, Berti G, Casati P. 1981. Sulfur and oxygen isotopes in Italian marine sulfates of Permian and Triassic ages. *Chem. Geol.* 34:65–79
- Cui Y, Kump LR, Ridgwell AJ, Charles AJ, Junium CK, et al. 2011. Slow release of fossil carbon during the Palaeocene-Eocene Thermal Maximum. *Nat. Geosci.* 4:481–85
- Erwin DH. 1993. *The Great Paleozoic Crisis: Life and Death in the Permian*. New York: Columbia Univ. Press. 327 pp.
- Erwin DH. 2006. *Extinction: How Life on Earth Nearly Ended 250 Million Years Ago*. Princeton, NJ: Princeton Univ. Press. 306 pp.
- Erwin DH, Bowring SA, Jin Y. 2002. End-Permian mass extinctions: a review. *Geol. Soc. Am. Spec. Pap.* 356:363–83
- Farabegoli E, Perri MC, Posenato R. 2007. Environmental and biotic changes across the Permian-Triassic boundary in western Tethys: the Bulla parastratotype, Italy. *Global Planet. Change* 55:109–35
- Farley KA, Mukhopadhyay S. 2001. An extraterrestrial impact at the Permian-Triassic boundary? *Science* 293:2343
- Farley KA, Ward P, Garrison G, Mukhopadhyay S. 2005. Absence of extraterrestrial  $^3\text{He}$  in Permian-Triassic age sedimentary rocks. *Earth Planet. Sci. Lett.* 240:265–75
- Feng Q, He W, Gu S, Meng Y, Jin Y, Zhang F. 2007. Radiolarian evolution during the latest Permian in South China. *Global Planet. Change* 55:177–92

- Fenton S, Grice K, Twitchett RJ, Böttcher ME, Looy CV, Nabbefeld B. 2007. Changes in biomarker abundances and sulfur isotopes of pyrite across the Permian-Triassic (P/Tr) Schuchert Dal section (East Greenland). *Earth Planet. Sci. Lett.* 262:230–39
- Flügel E. 2002. Triassic reef patterns. *Soc. Sediment. Geol. Spec. Publ.* 72:391–464
- Flügel E, Kiessling W. 2002. Patterns of Phanerozoic reef crises. *Soc. Sediment. Geol. Spec. Publ.* 72:691–733
- Foster CB, Stephenson MH, Marshall C, Logan GA, Greenwood PF. 2002. A revision of *Reduviasporonites* Wilson 1962: description, illustration, comparison and biological affinities. *Palynology* 26:35–58
- Fraiser ML, Bottjer DJ. 2005. Restructuring in benthic level-bottom shallow marine communities due to prolonged environmental stress following the end-Permian mass extinction. *C. R. Palevol* 4:515–23
- Fraiser ML, Bottjer DJ. 2007. Elevated atmospheric CO<sub>2</sub> and the delayed biotic recovery from the end-Permian extinction. *Palaeogeogr. Palaeoclimatol. Palaeoecol.* 252:164–75
- French BM, Koeberl C. 2010. The convincing identification of terrestrial meteorite impact structures: what works, what doesn't, and why. *Earth-Sci. Rev.* 98:123–70
- Fröbisch J. 2008. Global taxonomic diversity of anomodonts (Tetrapoda, Therapsida) and the terrestrial rock record across the Permian-Triassic boundary. *PLoS ONE* 3(11):e3733
- Ganino C, Arndt NT. 2009. Climate changes caused by degassing of sediments during the emplacement of large igneous provinces. *Geology* 37:323–26
- Gastaldo RA, Neveling J, Clark CK, Newbury SS. 2009. The terrestrial Permian-Triassic boundary event bed is a nonevent. *Geology* 37:199–202
- Gorjan P, Kaiho K, Kakegawa T, Niitsuma S, Chen Z-Q, et al. 2007. Paleoredox, biotic and sulfur-isotopic changes associated with the end-Permian mass extinction in the western Tethys. *Chem. Geol.* 244:483–92
- Granier B, Grgasovic T. 2000. Les algues Dasycladales du Permien et du Trias. Nouvelle tentative d'inventaire bibliographique, géographique et stratigraphique. *Geol. Croat.* 53:1–197
- Grice K, Cao C-Q, Love GD, Böttcher ME, Twitchett RJ, et al. 2005. Photic zone euxinia during the Permian-Triassic superanoxic event. *Science* 307:706–9
- Grice K, Nabbefeld B, Maslen E. 2007. Source and significance of selected polycyclic aromatic hydrocarbons in sediments (Hovea-3 well, Perth Basin, Western Australia) spanning the Permian-Triassic boundary. *Org. Geochem.* 38:1795–803
- Grossman EL, Yancey TE, Jones TE, Bruckschen P, Chuvashov B, et al. 2008. Glaciation, aridification, and carbon sequestration in the Permo-Carboniferous: the isotopic record from low latitudes. *Palaeogeogr. Palaeoclimatol. Palaeoecol.* 268:222–33
- Groves JR, Altiner D. 2005. Survival and recovery of calcareous foraminifera pursuant to the end-Permian mass extinction. *C. R. Palevol* 4:419–32
- Groves JR, Altiner D, Rettori R. 2005. Extinction, survival, and recovery of lagenide foraminifers in the Permian-Triassic boundary interval, central Taurides, Turkey. *J. Paleontol.* 79(sp62):1–38
- Groves JR, Rettori R, Payne JL, Boyce MD, Altiner D. 2007. End-Permian mass extinction of lagenide foraminifers in the southern Alps (northern Italy). *J. Paleontol.* 81:415–34
- Hallam A. 1991. Why was there a delayed radiation after the end-Paleozoic extinctions? *Hist. Biol.* 5:257–62
- Harfoot MB, Pyle JA, Beerling DJ. 2008. End-Permian ozone shield unaffected by oceanic hydrogen sulphide and methane releases. *Nat. Geosci.* 1:247–52
- Hochuli PA, Hermann E, Vigran JO, Bucher H, Weissert H. 2010. Rapid demise and recovery of plant ecosystems across the end-Permian extinction event. *Global Planet. Change* 74:144–155
- Holser WT, Schonlaub HP, Attrep M, Boeckelmann K, Klein P, et al. 1989. A unique geochemical record at the Permian/Triassic boundary. *Nature* 337:39–44
- Horacek M, Brandner R, Richoz S, Povoden-Karadeniz E. 2010. Lower Triassic sulphur isotope curve of marine sulphates from the Dolomites, N-Italy. *Palaeogeogr. Palaeoclimatol. Palaeoecol.* 290:65–70
- Isozaki Y. 1997. Permo-Triassic boundary superanoxia and stratified superocean: records from lost deep sea. *Science* 276:235–38
- Ji Z, Yao J, Isozaki Y, Matsuda T, Wu G. 2007. Conodont biostratigraphy across the Permian-Triassic boundary at Chaotian, in northern Sichuan, China. *Palaeogeogr. Palaeoclimatol. Palaeoecol.* 252:39–55
- Jin YG, Zhang J, Shang QH. 1994. Two phases of the end-Permian mass extinction. In *Pangea: Global Environments and Resources*, ed. AF Embry, B Beauchamp, DJ Glass, pp. 813–22. Calgary, Can.: Can. Soc. Pet. Geol.

- Kaiho K, Kajiwar Y, Nakano T, Miura Y, Kawahata H, et al. 2001. End-Permian catastrophe by a bolide impact: evidence of a gigantic release of sulfur from the mantle. *Geology* 29:815–18
- Kajiwar Y, Yamakita S, Ishida K, Ishiga H, Imai A. 1994. Development of a largely anoxic stratified ocean and its temporary massive mixing at the Permian-Triassic boundary supported by the sulfur isotopic record. *Palaeogeogr. Palaeoclimatol. Palaeoecol.* 111:367–79
- Kamo SL, Czamanske GK, Amelin Y, Fedorenko VA, Davis DW, Trofimov VR. 2003. Rapid eruption of Siberian flood-volcanic rocks and evidence for coincidence with the Permian-Triassic boundary and mass extinction at 251 Ma. *Earth Planet. Sci. Lett.* 214:75–91
- Kampschulte A, Strauss H. 2004. The sulfur isotopic evolution of Phanerozoic seawater based on the analysis of structurally substituted sulfate in carbonates. *Chem. Geol.* 204:255–86
- Kershaw S, Crasquin S, Li Y, Collin P-Y, Forel M-B, et al. 2012. Microbialites and global environmental change across the Permian-Triassic boundary: a synthesis. *Geobiology* 10:25–47
- Kershaw S, Li Y, Crasquin-Soleau S, Feng Q, Mu X, et al. 2007. Earliest Triassic microbialites in the South China block and other areas: controls on their growth and distribution. *Facies* 53:409–25
- Kiessling W, Simpson C. 2011. On the potential for ocean acidification to be a general cause of ancient reef crises. *Global Change Biol.* 17:56–67
- Knoll AH, Bambach RK, Canfield DE, Grotzinger JP. 1996. Comparative Earth history and Late Permian mass extinction. *Science* 273:452–57
- Knoll AH, Bambach RK, Payne JL, Pruss S, Fischer WW. 2007. Paleophysiology and end-Permian mass extinction. *Earth Planet. Sci. Lett.* 256:295–313
- Koeberl C, Farley KA, Peucker-Ehrenbrink B, Sephton MA. 2004. Geochemistry of the end-Permian extinction event in Austria and Italy: no evidence for an extraterrestrial component. *Geology* 32:1053–56
- Korte C, Kozur HW. 2010. Carbon-isotope stratigraphy across the Permian-Triassic boundary: a review. *J. Asian Earth Sci.* 39:215–35
- Korte C, Kozur HW, Joachimski MM, Strauss H, Veizer J, Schwark L. 2004. Carbon, sulfur, oxygen and strontium isotope records, organic geochemistry and biostratigraphy across the Permian/Triassic boundary in Abadeh, Iran. *Int. J. Earth Sci.* 93:565–81
- Kozur HW. 1998. Some aspects of the Permian-Triassic boundary (PTB) and of the possible causes for the biotic crisis around this boundary. *Palaeogeogr. Palaeoclimatol. Palaeoecol.* 143:227–72
- Kozur HW. 2007. Biostratigraphy and event stratigraphy in Iran around the Permian-Triassic Boundary (PTB): implications for the causes of the PTB biotic crisis. *Global Planet. Change* 55:155–76
- Krull ES, Lehrmann DJ, Druke D, Kessel B, Yu YY, Li RX. 2004. Stable carbon isotope stratigraphy across the Permian-Triassic boundary in shallow marine carbonate platforms, Nanpanjiang Basin, south China. *Palaeogeogr. Palaeoclimatol. Palaeoecol.* 204:297–315
- Kump LR, Pavlov A, Arthur MA. 2005. Massive release of hydrogen sulfide to the surface ocean and atmosphere during intervals of oceanic anoxia. *Geology* 33:397–400
- Lehrmann DJ, Payne JL, Felix SV, Dilleit PM, Wang H, et al. 2003. Permian-Triassic boundary sections from shallow marine carbonate platforms of the Nanpanjiang Basin, south China: implications for oceanic conditions associated with the end-Permian extinction and its aftermath. *Palaos* 18:138–52
- Leighton LR, Schneider CL. 2008. Taxon characteristics that promote survivorship through the Permian-Triassic interval: transition from the Paleozoic to the Mesozoic brachiopod fauna. *Paleobiology* 34:65–79
- Luo G, Kump LR, Wang Y, Tong J, Arthur MA, et al. 2010. Isotopic evidence for an anomalously low oceanic sulfate concentration following end-Permian mass extinction. *Earth Planet. Sci. Lett.* 300:101–11
- Luo G, Wang Y, Algeo TJ, Kump LR, Bai X, et al. 2011. Enhanced nitrogen fixation in the immediate aftermath of the latest Permian marine mass extinction. *Geology* 39:647–50
- Maxwell WD. 1992. Permian and Early Triassic extinction of non-marine tetrapods. *Palaeontology* 35:571–83
- McArthur JM, Howarth RJ, Bailey TR. 2001. Strontium isotope stratigraphy: LOWESS version 3: best fit to the marine Sr-isotope curve for 0–509 Ma and accompanying lookup table for derived numerical age. *J. Geol.* 109:155–70
- Meyer KM, Jost AB, Yu M, Payne JL. 2011.  $\delta^{13}\text{C}$  evidence that high primary productivity delayed recovery from end-Permian mass extinction. *Earth Planet. Sci. Lett.* 302:278–84



- Meyer KM, Kump LR. 2008. Oceanic euxinia in Earth history: causes and consequences. *Annu. Rev. Earth Planet. Sci.* 36:251–88
- Meyer KM, Kump LR, Ridgwell A. 2008. Biogeochemical controls on photic-zone euxinia during the end-Permian mass extinction. *Geology* 36:747–50
- Mundil R, Ludwig KR, Metcalfe I, Renne PR. 2004. Age and timing of the Permian mass extinctions: U/Pb dating of closed-system zircons. *Science* 305:1760–63
- Nakazawa K, Kapoor HM, Ishii K, Bando Y, Okimura Y, Tokuoka T. 1975. The Upper Permian and the Lower Triassic in Kashmir, India. *Mem. Fac. Sci. Kyoto Univ. Ser. Geol. Mineral.* 42:1–106
- Newell ND. 1962. Paleontological gaps and geochronology. *J. Paleontol.* 36:592–610
- Newton RJ, Pevitt EL, Wignall PB, Bottrell SH. 2004. Large shifts in the isotopic composition of seawater sulphate across the Permo-Triassic boundary in northern Italy. *Earth Planet. Sci. Lett.* 218:331–45
- Nielsen JK, Shen Y, Piasecki S, Stemmerik L. 2010. No abrupt change in redox condition caused the end-Permian marine ecosystem collapse in the East Greenland Basin. *Earth Planet. Sci. Lett.* 291:32–38
- Payne JL, Finnegan S. 2007. The effect of geographic range on extinction risk during background and mass extinction. *Proc. Natl. Acad. Sci. USA* 104:10506–11
- Payne JL, Lehrmann DJ, Follett D, Seibel M, Kump LR, et al. 2007. Erosional truncation of uppermost Permian shallow-marine carbonates and implications for Permian-Triassic boundary events. *Geol. Soc. Am. Bull.* 119:771–84
- Payne JL, Lehrmann DJ, Wei JY, Orchard MJ, Schrag DP, Knoll AH. 2004. Large perturbations of the carbon cycle during recovery from the end-Permian extinction. *Science* 305:506–9
- Payne JL, Turchyn AV, Paytan A, DePaolo DJ, Lehrmann DJ, et al. 2010. Calcium isotope constraints on the end-Permian mass extinction. *Proc. Natl. Acad. Sci. USA* 107:8543–48
- Phillips J. 1860. *Life on Earth: Its Origin and Succession*. London: Macmillan
- Posenato R. 2009. Survival patterns of macrobenthic marine assemblages during the end-Permian mass extinction in the western Tethys (Dolomites, Italy). *Palaeogeogr. Palaeoclimatol. Palaeoecol.* 280:150–67
- Posenato R. 2010. Marine biotic events in the Lopingian succession and latest Permian extinction in the Southern Alps (Italy). *Geol. J.* 45:195–215
- Powers CM, Pachut JF. 2008. Diversity and distribution of Triassic bryozoans in the aftermath of the end-Permian mass extinction. *J. Paleontol.* 82:362–71
- Pruss SB, Bottjer DJ. 2004. Late Early Triassic microbial reefs of the western United States: a description and model for their deposition in the aftermath of the end-Permian mass extinction. *Palaeogeogr. Palaeoclimatol. Palaeoecol.* 211:127–37
- Rampino MR, Adler AC. 1998. Evidence for abrupt latest Permian mass extinction of foraminifera: results of tests for the Signor-Lipps effect. *Geology* 26:415–18
- Rampino MR, Caldeira K. 2005. Major perturbation of ocean chemistry and a ‘Strangelove Ocean’ after the end-Permian mass extinction. *Terra Nova* 17:554–59
- Rees PM. 2002. Land-plant diversity and the end-Permian mass extinction. *Geology* 30:827–30
- Reichow MK, Pringle MS, Al’Mukhamedov AI, Allen MB, Andreichev VL, et al. 2009. The timing and extent of the eruption of the Siberian Traps large igneous province: implications for the end-Permian environmental crisis. *Earth Planet. Sci. Lett.* 277:9–20
- Reichow MK, Saunders AD, White RV, Pringle MS, Al’Mukhamedov AI, et al. 2002. <sup>40</sup>Ar/<sup>39</sup>Ar dates from the West Siberian Basin: Siberian flood basalt province doubled. *Science* 296:1846–49
- Renne PR, Black MT, Zhang Z, Richards MA, Basu AR. 1995. Synchrony and causal relations between Permian-Triassic boundary crises and Siberian flood volcanism. *Science* 269:1413–16
- Renne PR, Melosh HJ, Farley KA, Reimold WU, Koeberl C, et al. 2004. Is Bedout an impact crater? Take 2. *Science* 306:610–12
- Rhodes MC, Thayer CW. 1991. Mass extinctions: ecological selectivity and primary production. *Geology* 19:877–80
- Riccardi A, Arthur MA, Kump LR. 2006. Sulfur isotopic evidence for chemocline upward excursions during the end-Permian mass extinction. *Geochim. Cosmochim. Acta* 70:5740–52
- Rothman D. 2010. *Singular blow-up in the end-Permian carbon cycle*. Presented at Fall Meet., AGU, Dec. 13–17, San Francisco (Abstr. B53B-08)

- Ryskin G. 2003. Methane-driven oceanic eruptions and mass extinctions. *Geology* 31:741–44
- Sano H, Kuwahara K, Yao A, Agematsu S. 2010. Panthalassan seamount-associated Permian-Triassic boundary siliceous rocks, Mino Terrane, central Japan. *Paleontol. Res.* 14:293–314
- Schindewolf OH. 1954. Ueber die moeglichen Ursachen der grossen erdgeschichtlichen Faunenschnitte. *Neues Jahrb. Geol. Palaeontol. Monatshefte* 10:457–65
- Schulte P, Alegret L, Arenillas I, Arz JA, Barton PJ, et al. 2010. The Chicxulub asteroid impact and mass extinction at the Cretaceous-Paleogene boundary. *Science* 327:1214–18
- Şengör AMC, Atayman S. 2009. The Permian extinction and the Tethys: an exercise in global geology. *Geol. Soc. Am. Spec. Pap.* 448:1–85
- Sephton MA, Looy CV, Brinkhuis H, Wignall PB, de Leeuw JW, Visscher H. 2005. Catastrophic soil erosion during the end-Permian biotic crisis. *Geology* 33:941–44
- Sepkoski JJ. 1981. A factor analytic description of the Phanerozoic marine fossil record. *Paleobiology* 7:36–53
- Sepkoski JJ. 2002. *A Compendium of Fossil Marine Animal Genera*. Bull. Am. Paleontol. 363. Ithaca, NY: Paleontol. Res. Inst. 560 pp.
- Shen S-Z, Cao C-Q, Henderson CM, Wang X-D, Shi GR, et al. 2006. End-Permian mass extinction pattern in the northern peri-Gondwanan region. *Palaeoworld* 15:3–30
- Shen S-Z, Cao C-Q, Zhang Y, Li W, Shi GR, et al. 2010a. End-Permian mass extinction and palaeoenvironmental changes in Neotethys; evidence from an oceanic carbonate section in southwestern Tibet. *Global Planet. Change* 73:3–14
- Shen S-Z, Crowley JL, Wang Y, Bowring SA, Erwin DH, et al. 2011. Calibrating the end-Permian mass extinction. *Science* 334:1367–72
- Shen S-Z, Henderson CM, Bowring SA, Cao C-Q, Wang Y, et al. 2010b. High-resolution Lopingian (Late Permian) timescale of South China. *Geol. J.* 45:122–34
- Shen S-Z, Mei S-L. 2010. Lopingian (Late Permian) high-resolution conodont biostratigraphic framework in Iran. *Geol. J.* 45:135–61
- Shen W, Lin Y, Xu L, Li J, Wu Y, Sun Y. 2007. Pyrite framboids in the Permian-Triassic boundary section at Meishan, China: evidence for dysoxic deposition. *Palaeogeogr. Palaeoclimatol. Palaeoecol.* 2007:323–31
- Sheng J-Z, Chen C-Z, Wang Y-G, Rui L, Liao Z-T, et al. 1984. Permian-Triassic boundary in middle and eastern Tethys. *J. Fac. Sci. Hokkaido Univ. Ser. 4: Geol. Mineral.* 21:133–81
- Stanley SM, Yang X. 1994. A double mass extinction at the end of the Paleozoic Era. *Science* 266:1340–44
- Steele-Petrović HM. 1979. The physiological differences between articulate brachiopods and filter-feeding bivalves as a factor in the evolution of marine level-bottom communities. *Palaeontology* 22:101–34
- Svensen H, Planke S, Mørch-Sørensen A, Jamveit B, Myklebust R, et al. 2004. Release of methane from a volcanic basin as a mechanism for initial Eocene global warming. *Nature* 429:542–45
- Svensen H, Planke S, Polozov AG, Schmidbauer N, Corfu F, et al. 2009. Siberian gas venting and the end-Permian environmental crisis. *Earth Planet. Sci. Lett.* 277:490–500
- Thomas BM, Willink RJ, Grice K, Twitchett RJ, Purcell RR, et al. 2004. Unique marine Permian-Triassic boundary section from Western Australia. *Aust. J. Earth Sci.* 51:423–30
- Twitchett RJ, Looy CV, Morante R, Visscher H, Wignall PB. 2001. Rapid and synchronous collapse of marine and terrestrial ecosystems during the end-Permian biotic crisis. *Geology* 29:351–54
- Twitchett RJ, Oji T. 2005. Early Triassic recovery of echinoderms. *C. R. Palevol* 4:463–74
- Visscher H, Brinkhuis H, Dilcher DL, Elsik WC, Eshet Y, et al. 1996. The terminal Paleozoic fungal event: evidence of terrestrial ecosystem destabilization and collapse. *Proc. Natl. Acad. Sci. USA* 93:2155–58
- Visscher H, Looy CV, Collinson ME, Brinkhuis H, Cittert J, et al. 2004. Environmental mutagenesis during the end-Permian ecological crisis. *Proc. Natl. Acad. Sci. USA* 101:12952–56
- Visscher H, Sephton MA, Looy CV. 2011. Fungal virulence at the time of the end-Permian biosphere crisis? *Geology* 39:883–86
- Wang C, Visscher H. 2007. Abundance anomalies of aromatic biomarkers in the Permian-Triassic boundary section at Meishan, China—evidence of end-Permian terrestrial ecosystem collapse. *Palaeogeogr. Palaeoclimatol. Palaeoecol.* 252:291–303
- Ward PD, Botha J, Buick R, De Kock MO, Erwin DH, et al. 2005. Abrupt and gradual extinction among Late Permian land vertebrates in the Karoo Basin, South Africa. *Science* 307:709–14



- Welander PV, Coleman ML, Sessions AL, Summons RE, Newman DK. 2010. Identification of a methylase required for 2-methylhopanoid production and implications for the interpretation of sedimentary hopanes. *Proc. Natl. Acad. Sci. USA* 107:8537–42
- Wignall P, Thomas B, Willink R, Watling J. 2004. Is Bedout an impact crater? Take 1. *Science* 306:609–10
- Wignall PB. 2001. Large igneous provinces and mass extinctions. *Earth-Sci. Rev.* 53:1–33
- Wignall PB, Hallam A. 1992. Anoxia as a cause of the Permian/Triassic mass extinction: facies evidence from northern Italy and the western United States. *Palaeogeogr. Palaeoclimatol. Palaeoecol.* 93:21–46
- Wignall PB, Hallam A. 1993. Griesbachian (Earliest Triassic) paleoenvironmental changes in the Salt Range, Pakistan and southeast China and their bearing on the Permo-Triassic mass extinction. *Palaeogeogr. Palaeoclimatol. Palaeoecol.* 102:215–37
- Wignall PB, Morante R, Newton R. 1998. The Permo-Triassic transition in Spitsbergen:  $\delta^{13}\text{C}_{\text{org}}$  chemostratigraphy, Fe and S geochemistry, facies, fauna and trace fossils. *Geol. Mag.* 135:47–62
- Wignall PB, Newton R, Brookfield ME. 2005. Pyrite framboid evidence for oxygen-poor deposition during the Permian-Triassic crisis in Kashmir. *Palaeogeogr. Palaeoclimatol. Palaeoecol.* 216:183–88
- Wignall PB, Twitchett RJ. 1996. Oceanic anoxia and the end-Permian mass extinction. *Science* 272:1155–58
- Wignall PB, Twitchett RJ. 2002. Extent, duration, and nature of the Permian-Triassic superanoxic event. *Geol. Soc. Am. Spec. Publ.* 356:395–413
- Xie SC, Pancost RD, Huang J, Wignall PB, Yu J, et al. 2007. Change in the global carbon cycle occurred as two episodes during the Permian-Triassic crisis. *Geology* 35:1083–86
- Xie SC, Pancost RD, Yin HF, Wang HM, Evershed RP. 2005. Two episodes of microbial change coupled with Permo/Triassic faunal mass extinction. *Nature* 434:494–97
- Xiong CH, Wang Q. 2011. Permian-Triassic land plant diversity in South China: was there a mass extinction at the Permian/Triassic boundary? *Paleobiology* 37:157–167
- Yin HF, Feng QL, Lai XL, Baud A, Tong JN. 2007. The protracted Permo-Triassic crisis and multi-episode extinction around the Permian-Triassic boundary. *Global Planet. Change* 55:1–20

# Contents

Reminiscences From a Career in Geomicrobiology <i>Henry L. Ehrlich</i> .....	1
Mixing and Transport of Isotopic Heterogeneity in the Early Solar System <i>Alan P. Boss</i> .....	23
Tracing Crustal Fluids: Applications of Natural $^{129}\text{I}$ and $^{36}\text{Cl}$ <i>Udo Fehn</i> .....	45
SETI@home, BOINC, and Volunteer Distributed Computing <i>Eric J. Korpela</i> .....	69
End-Permian Mass Extinction in the Oceans: An Ancient Analog for the Twenty-First Century? <i>Jonathan L. Payne and Matthew E. Clapham</i> .....	89
Magma Oceans in the Inner Solar System <i>Linda T. Elkins-Tanton</i> .....	113
History of Seawater Carbonate Chemistry, Atmospheric $\text{CO}_2$ , and Ocean Acidification <i>Richard E. Zeebe</i> .....	141
Biomimetic Properties of Minerals and the Search for Life in the Martian Meteorite ALH84001 <i>Jan Martel, David Young, Hsin-Hsin Peng, Cheng-Yeu Wu, and John D. Young</i> ....	167
Archean Subduction: Fact or Fiction? <i>Jeroen van Hunen and Jean-François Moyen</i> .....	195
Molecular Paleohydrology: Interpreting the Hydrogen-Isotopic Composition of Lipid Biomarkers from Photosynthesizing Organisms <i>Dirk Sachse, Isabelle Billault, Gabriel J. Bowen, Yoshito Chikaraishi, Todd E. Dawson, Sarah J. Feakins, Katherine H. Freeman, Clayton R. Magill, Francesca A. McNerney, Marcel T.J. van der Meer, Pratigya Polissar, Richard J. Robins, Julian P. Sachs, Hanns-Ludwig Schmidt, Alex L. Sessions, James W.C. White, Jason B. West, and Ansgar Kabmen</i> .....	221

Building Terrestrial Planets <i>A. Morbidelli, J.I. Lunine, D.P. O'Brien, S.N. Raymond, and K.J. Walsh</i>	251
Paleontology of Earth's Mantle <i>Norman H. Sleep, Dennis K. Bird, and Emily Pope</i>	277
Molecular and Fossil Evidence on the Origin of Angiosperms <i>James A. Doyle</i>	301
Infrasound: Connecting the Solid Earth, Oceans, and Atmosphere <i>M.A.H. Hedlin, K. Walker, D.P. Drob, and C.D. de Groot-Hedlin</i>	327
Titan's Methane Weather <i>Henry G. Roe</i>	355
Extratropical Cooling, Interhemispheric Thermal Gradients, and Tropical Climate Change <i>John C.H. Chiang and Andrew R. Friedman</i>	383
The Role of H <sub>2</sub> O in Subduction Zone Magmatism <i>Timothy L. Grove, Christy B. Till, and Michael J. Krawczynski</i>	413
Satellite Geomagnetism <i>Nils Olsen and Claudia Stolle</i>	441
The Compositions of Kuiper Belt Objects <i>Michael E. Brown</i>	467
Tectonics of the New Guinea Region <i>Suzanne L. Baldwin, Paul G. Fitzgerald, and Laura E. Webb</i>	495
Processes on the Young Earth and the Habitats of Early Life <i>Nicholas T. Arndt and Euan G. Nisbet</i>	521
The Deep, Dark Energy Biosphere: Intraterrestrial Life on Earth <i>Katrina J. Edwards, Keir Becker, and Frederick Colwell</i>	551
Geophysics of Chemical Heterogeneity in the Mantle <i>Lars Stixrude and Carolina Lithgow-Bertelloni</i>	569
The Habitability of Our Earth and Other Earths: Astrophysical, Geochemical, Geophysical, and Biological Limits on Planet Habitability <i>Charles H. Lineweaver and Aditya Chopra</i>	597
The Future of Arctic Sea Ice <i>Wieslaw Maslowski, Jaclyn Clement Kinney, Matthew Higgins, and Andrew Roberts</i>	625
The Mississippi Delta Region: Past, Present, and Future <i>Michael D. Blum and Harry H. Roberts</i>	655

Climate Change Impacts on the Organic Carbon Cycle at the Land-Ocean Interface <i>Elizabeth A. Canuel, Sarah S. Cammer, Hadley A. McIntosh, and Christina R. Pondell</i> .....	685
--	-----

## Indexes

Cumulative Index of Contributing Authors, Volumes 31–40 .....	713
Cumulative Index of Chapter Titles, Volumes 31–40 .....	717

## Errata

An online log of corrections to *Annual Review of Earth and Planetary Sciences* articles  
may be found at <http://earth.annualreviews.org>